CMLS, Cell. Mol. Life Sci. 62 (2005) 1038–1046
1420-682X/05/091038-09
DOI 10.1007/s00018-005-4547-z

CMLS Cellular and Molecular Life Sciences

Research Article

Structural organization and cellular localization of tuftelin-interacting protein 11 (TFIP11)

X. Wen [a], Y.-P. Lei [a], Y. L. Zhou [a], C. T. Okamoto [b], M. L. Snead [a] and M. L. Paine [a, *]

[a] University of Southern California School of Dentistry, Center for Craniofacial Molecular Biology, 2250 Alcazar Street, CSA room 103, Los Angeles, California 90033-1004 (USA), e-mail: paine@usc.edu
[b] University of Southern California School of Pharmacy, Department of Pharmaceutical Sciences, Los Angeles, California 90089-9121 (USA)

Received 8 December 2004; received after revision 27 January 2005; accepted 8 March 2004

Abstract. Tuftelin-interacting protein (TFIP11) was first identified in a yeast two-hybrid screening as a protein interacting with tuftelin. The ubiquitous expression of TFIP11 suggested that it might have other functions in non-dental tissues. TFIP11 contains a G-patch, a protein domain believed to be involved in RNA binding. Using a green fluorescence protein tag, TFIP11 was found to locate in a novel subnuclear structure that we refer to as the TFIP body. An in vivo splicing assay demonstrated that TFIP11 is a novel splicing factor. TFIP11 diffuses from the TFIP body following RNase A treatment, suggesting that the retention of TFIP11 is RNA dependent. RNA polymerase II inhibitor (-amanitin and actinomycin D) treatment causes enlargement in size and decrease in number of TFIP bodies, suggesting that TFIP bodies perform a storage function rather than an active splicing function. The TFIP body may therefore represent a new subnuclear storage compartment for splicing components.

Key words. Alternative splicing; G-patch; green-fluorescence protein; RNA splicing; spliceosome; TFIP11; TFIP body; TIP39; TIP39kDa; tuftelin-interacting protein.

Tuftelin-interacting protein (TFIP11) was first identified in a yeast two-hybrid screening as a protein interacting with tuftelin, one of the presumed enamel matrix proteins. We proposed mouse TFIP11 (mTFIP11, named TIP39 at that time) to be involved in the secretory pathway of extracellular proteins [1]. The symbol TFIP11 (tuftelin-interacting protein 11) has recently been assigned to the mouse gene by the HUGO Gene Nomenclature Committee. The TFIP11 gene is located on mouse chromosome 5F and human chromosome 22q12.1.

Tuftelin, an acidic protein, was first cloned by screening a tooth-enriched gene expression library with polyclonal antibodies against a gel-purified 66-kDa enamelin protein [2]. Tuftelin has since been considered a member of the enamel matrix proteins and proposed to be involved in mineralization. However, a role for tuftelin in enamel organic matrix formation has not yet been demonstrated. Unlike other protein members of enamel, which are expressed only in tooth tissues and have a signal peptide directing the secretory proteins to the matrix, tuftelin does not have a recognizable signal peptide. Tuftelin is also expressed in a large number of non-dental tissues, such as kidney, liver, lung, and testis [3]. TFIP11 displays a simi-

* Corresponding author.
The nucleotide sequence for the cDNA to mouse TFIP11 (previously known as TIP39 and TIP39kDa) has been submitted to GenBank™ / EBI Data Bank with accession numbers AF290474 and NM_018783. The accession number for the human TFIP11 homologue is NM_012143.

lar tissue expression profile as tuftelin. Expression of tuftelin and TFIP11 in non-mineralizing tissues suggests that both genes may have a fundamental role in cell biology, in addition to any role they may play in mineralization.

The human homologue of TFIP11 (hTFIP11) is 92% identical to mTFIP11 at the protein level [1]. Recently, hTFIP11 was identified as a potential spliceosomal protein in a proteomic study intending to identify the complete set of proteins that constitute intact functional spliceosomes [4]. In addition, hTFIP11 was identified in the spliceosome by other proteomic studies by different groups [5]. In lower organisms, a clear homologue of TFIP11 is not evident, although the yeast protein YLR424w [6] contains the G-patch domain and this protein is required for cell viability. Taken together, these results suggest a possible role for TFIP11 and/or G-patch-containing proteins in mRNA splicing.

The cell nucleus is highly compartmentalized. The subnuclear structures including nucleoli, splicing speckles, Cajal bodies, gems, PML bodies and paraspeckles are not enclosed by membranes, yet are distinct from the surrounding nucleoplasm [7–10]. Many nuclear proteins involved in different nuclear activities, such as ribosome biogenesis, transcription, and RNA splicing, are known to interact dynamically with these subnuclear structures. Disruption of the subnuclear organization can result in defects in cell functions and may cause molecular diseases. For example, PML and Cajal bodies have been found to be associated with genetic diseases. They either diminish in number or disaggregate in corresponding patient cells [7]. Many, but not all splicing factors are enriched in subnuclear structures termed 'speckles' (SC35 domains, or splicing factor compartment). The speckles (20–50 speckles per nucleus) are punctate, irregular shaped dynamic structures, corresponding to interchromatin granule clusters (IGCs) observed with electron microscopy, which have been proposed to be involved in splicing and splicing component storage/assembly/modification [9, 11]. Splicing is an event to remove introns from transcribed pre-mRNA in order to generate a functional message from the DNA template. Splicing is catalyzed by a 60S ribonucleoprotein complex referred to as the spliceosome consisting of pre-mRNA, five small nuclear RNAs (U1, U2, U4, U5, and U6) and about 145 proteins [10, 12]. The cis consensus sequence in pre-mRNA and the transacting proteins are the controlling elements.

In our study, using a green fluorescence protein (GFP)-fusion protein approach, TFIP11 was found to localize to a novel subnuclear structure, in close proximity to the SC35 speckles. The nuclear distribution of TFIP11 was sensitive to RNA polymerase II transcription inhibitors and RNase treatment. Increased expression of TFIP11 in cells resulted in changes in the E1A minigene [13] splicing pattern, which functionally demonstrated the involvement of TFIP11 in mRNA splicing.

Materials and methods

Cloning of full-length TFIP11

The entire 5′ region of TFIP11 was cloned using the FirstChoice RLM-RACE kit (Ambion) and two TFIP11-specific oligonucleotide primers. The RNA template was prepared from mouse testicle using RNA-Bee solution (Tel-Test). The RACE reaction conditions were as recommended in the kit. The 3′ TFIP11 region was as published under the clone TIP33 [14]. The overlap of the RACE product and the 3′ region was approximately 200 bp. The 5′ TFIP11 cDNA sequences from two independent RACE reactions were sequenced and identical sequence data were obtained. The overlapping region of the RACE product and 3′ TFIP11 matched exactly. A full-length cDNA was generated using PCR and appropriate restriction enzyme digestions and ligations. The complete mTFIP11 generated was sequenced entirely to ensure no cloning/PCR errors.

Plasmid constructs

Employing PCR and appropriate restriction enzyme digestion, mouse TFIP11 cDNA corresponding to the entire open-reading frame (ORF) of 838 amino acids minus the initial ATG was cloned into the vector pEGFP-C1, and the entire ORF minus the stop codon into pEGFP-N1 (Clontech). Resulting plasmids were named TFIP11-C1 and TFIP11-N1, respectively (fig. 1A). All PCR amplified regions were verified to be error free by sequencing the final clones.

Cell culture and transient transfection

Ameloblast-like LS8 cells were cultured as previously described [15]. HEK293 and Hela cells were maintained in Dulbecco's modification of Eagle's medium (DMEM) with high glucose (4.5 g/l) supplemented with 10% (v/v) fetal calf serum (FCS). For transient transfection assays, cells were grown on either glass cover slips in 3.5-cm cell culture dishes or on two-well chamber slides (Lab-Tek). Lipofectamine 2000 (Invitrogen) was used as the transfection reagent according to the manufacturer's instructions. Cells were fixed with 4% paraformaldehyde 24 h after transfection, washed with phosphate buffered saline (PBS), and mounted with Pro-Long anti-fade reagent (Molecular Probes). Images were taken from a ×63 Carl Zeiss planapo objective of an Olympus IMT-2 microscope and/or ×60 lens of a Nikon PCM2000 confocal system.

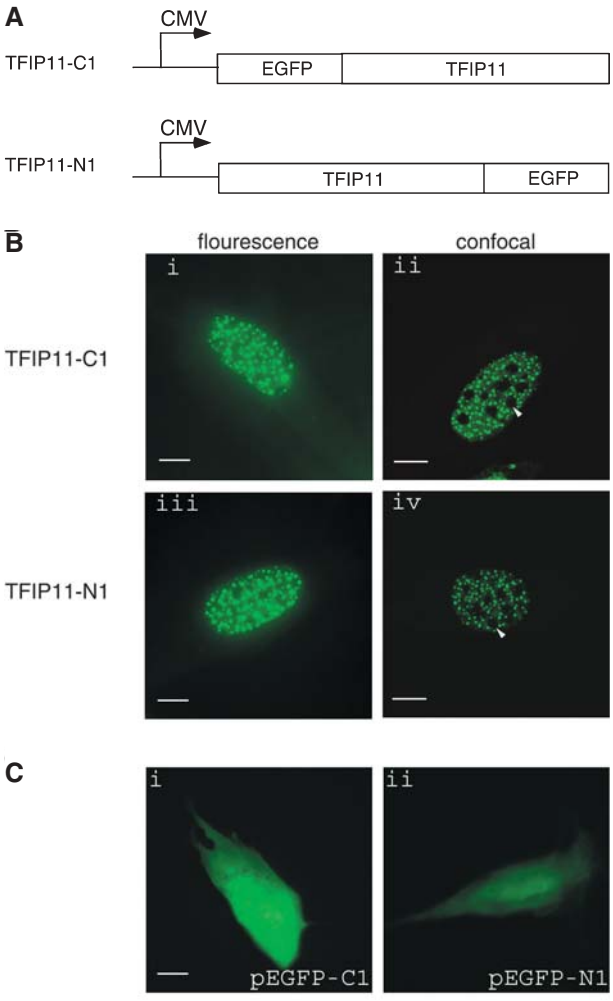

Figure 1. TFIP11-EGFP fusion constructs and subcellular localization of the fusion protein. (*A*) Schematic representation of two fusion constructs with TFIP11 fused to either the C terminus of EGFP (TFIP11-C1) or N terminus of EGFP (TFIP11-N1). (*B*) Subcellular localization of transiently expressed TFIP11-EGFP fusion protein in LS8 cells was determined by fluorescence (i, iii) and confocal microscopy (ii, iv). Arrowheads indicate nucleoli. Scale bar, 10 μm. (*C*) Localization of parental constructs, pEGFP-C1 (i) and pEGFP-N1 (ii), in transfected LS8 cells was determined by fluorescence microscope. Scale bar, 10 μm.

Immunofluorescence assay

Cells were first fixed with 2% paraformaldehyde/0.2% Triton X-100 for 10 min at room temperature (RT) and permeabilized with acetone for 5 min at −20 °C. Cells were then incubated with primary antibodies for 1 h at RT, washed with PBS three times, and incubated with secondary antibody for 1 h at RT. Finally, cells were washed with PBS three times and then mounted with the anti-fade reagent. The primary antibodies used were: anti-SC35 and anti-coilin antibodies (Sigma-Aldrich), anti-hnRNP antibody (Novus), anti-Sm antibody (Neomarkers), anti-PML antibody (Chemicon), anti-Sam68 antibody (BD Biosciences), and anti-paraspeckle protein 1 (PSP1) antibody [16]. The secondary antibodies were Texas Red-conjugated goat anti-mouse and goat anti-rabbit antibodies (Molecular Probes).

RNase digestion and transcription inhibitor treatment

Cells were fixed in methanol for 2 min at −20 °C 24 h after transfection, rinsed in PBS, and then incubated with RNase A (Sigma) at 100 μg/ml for 2 h at 37 °C. Cells were then washed and processed for fluorescence observations. For incubation of cells with drugs (Sigma-Aldrich), actinomycin D was added at a final concentration of 50 μg/ml or 0.04 μg/ml for 3 h, 5,6-dichloro-1-β-ribofuranosylbenzimidazole (DRB) at 75 μM for 3 h, cycloheximide at 100 μg/ml for 5 h, and α-amanitin at 50 μg/ml or 300 μg/ml for 5 h [17].

In vivo splicing assay

The assay was performed essentially as described previously [13]. The E1A minigene plasmid (1 μg) was transfected either alone or together with an increasing amount (0, 1, 2, 3, 4 μg) of TFIP11-N1 plasmid into LS8 cells in six-well plates. Parental vector pEGFP-N1 expressing EGFP protein was added to ensure that an equal amount of DNA was transfected. A control of 1 μg E1A and 4 μg empty pcDNA3 vector (Invitrogen) was also included to rule out any effect due to EGFP protein. RNA was isolated 24 h after transfection using an RNAqueous-4PCR kit (Ambion) as described in the manufacturer's instructions. For reverse transcription, 1 μg of isolated RNA was used as template and oligo-dT as primers with a Superscript first-strand synthesis system (Invitrogen). For PCR, 4 μl of the reverse transcription reaction (20 μl total) was used with a Taq PCR core kit (Qiagen). Denaturing, annealing, and extension were at 94 °C for 45 s, 55 °C for 45 s, and 72 °C for 45 s, respectively, using the primer pair 5′-cttttctcctccgagccgctccga-3′ (sense) and 5′-ctcaggatcaggtt cagacacagg-3′ (antisense). The bands were quantified using ImageQuant software (Molecular Dynamics).

Results

TFIP11 localized to a distinct punctate pattern in the nucleus

To determine the subcellular localization of TFIP11, two fusion constructs were generated with TFIP11 fused to either the C terminus of EGFP (TFIP11-C1) or N terminus of EGFP (TFIP11-N1) (fig. 1A), and transfected into LS8 cells individually. The images showed that both TFIP11-EGFP fusion proteins were mainly expressed as speckles in the nucleus but excluded from the nucleoli (fig. 1B). The parental EGFP control constructs (pEGFP-C1 and pEGFP-N1) were evenly expressed both in the cytoplasm

and nucleus (fig. 1C). These data implied that TFIP11 directs the speckled nuclear localization. The fact that the N-terminal fusion and C-terminal fusion gave identical results indicated that the fusion constructs likely recapitulated the endogenous TFIP11 localization. The distinct nuclear foci, referred to here as the TFIP body, varied in size (0.1–2 μm) and number (20–150). Some transfected cells showed large dots or large patches of the green signal and even some cytoplasm localization (unpublished data), which may suggest that an intrinsic cellular property, such as cell cycle status and transcriptional activity, affects the formation of these structures and distribution of TFIP11. HEK293, Hela, and MDCK cells showed an identical arrangement of TFIP bodies (data not shown).

TFIP11 localized to a novel subnuclear compartment

SC35 nuclear speckles are characteristic of those observed for known splicing factors. Recently, the complete set of human spliceosome proteins that constitute intact functional spliceosome have been studied [4]. The human homologue of TFIP11 protein is one of the novel proteins identified in functional spliceosomes. To examine whether TFIP11 colocalized with these nuclear speckles, a comparison with splicing factor SC35, which is now widely used as a marker protein for nuclear speckles, was performed [18]. HEK293 cells were transfected with TFIP11-N1 (fig. 2A) and stained with SC35 antibody (fig. 2A). A very similar, but not overlapping expression pattern was found for TFIP11 and SC35 (fig. 2A). High magnification of the image revealed that TFIP11 and SC35 protein were localized in foci that were in close proximity (fig. 2A). Both SC35 and TFIP11 were excluded from nucleoli.

Paraspeckles are a newly identified nuclear compartment in the interchromatin nucleoplamic space, adjacent to splicing speckles (SC35 speckles) [16]. To determine whether TFIP bodies were distinct from paraspeckles, HeLa cells were transiently transfected with TFIP11-C1 and immunostained with paraspeckle antibody (fig. 2B). The merged image showed that TFIP bodies were not colocalized with paraspeckles.

To further determine whether TFIP bodies colocalized with any other well known nuclear structures, such as Cajal bodies, snRNP, hnRNP, PML bodies, or the perinucle-

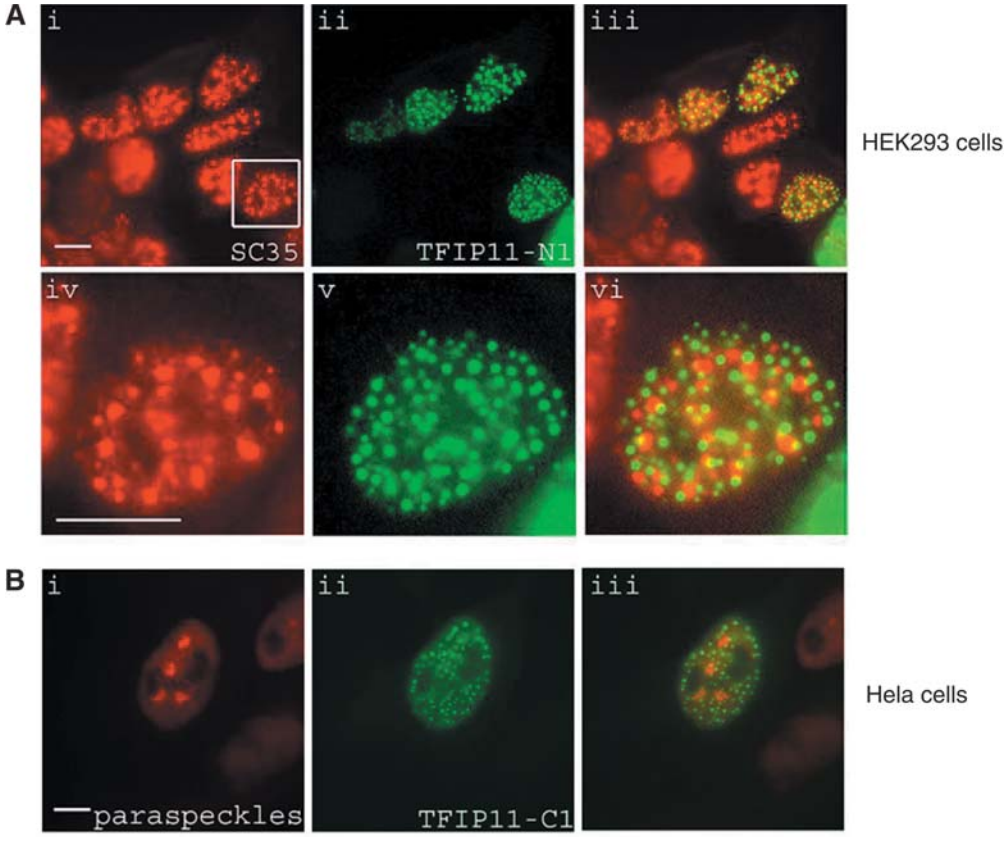

Figure 2. TFIP11 localized to a novel subnuclear compartment. Scale bar, 10 μm. (*A*) HEK293 cells were transfected with TFIP11-N1 (ii) and immunostained with antibody against SC35 (i). An overlay of the green-fluorescent image and the SC35 staining is shown in iii. iv shows an enlarged image of the boxed area in i. The corresponding enlarged green fluorescent and merged image are shown in v and vi. (*B*) HeLa cells were transfected with TFIP11-C1 (ii) and immunostained with antibody against paraspeckles (i). iii shows the merged image. (*C*) HEK293, LS8, and HeLa cells were transfected with TFIP11-N1 (the middle column) and immunostained with antibodies against various nuclear markers: coilin (i), Sm (iv), hnRNP (vii), PML (x), and Sam68 (xiii). The right column shows merged images.

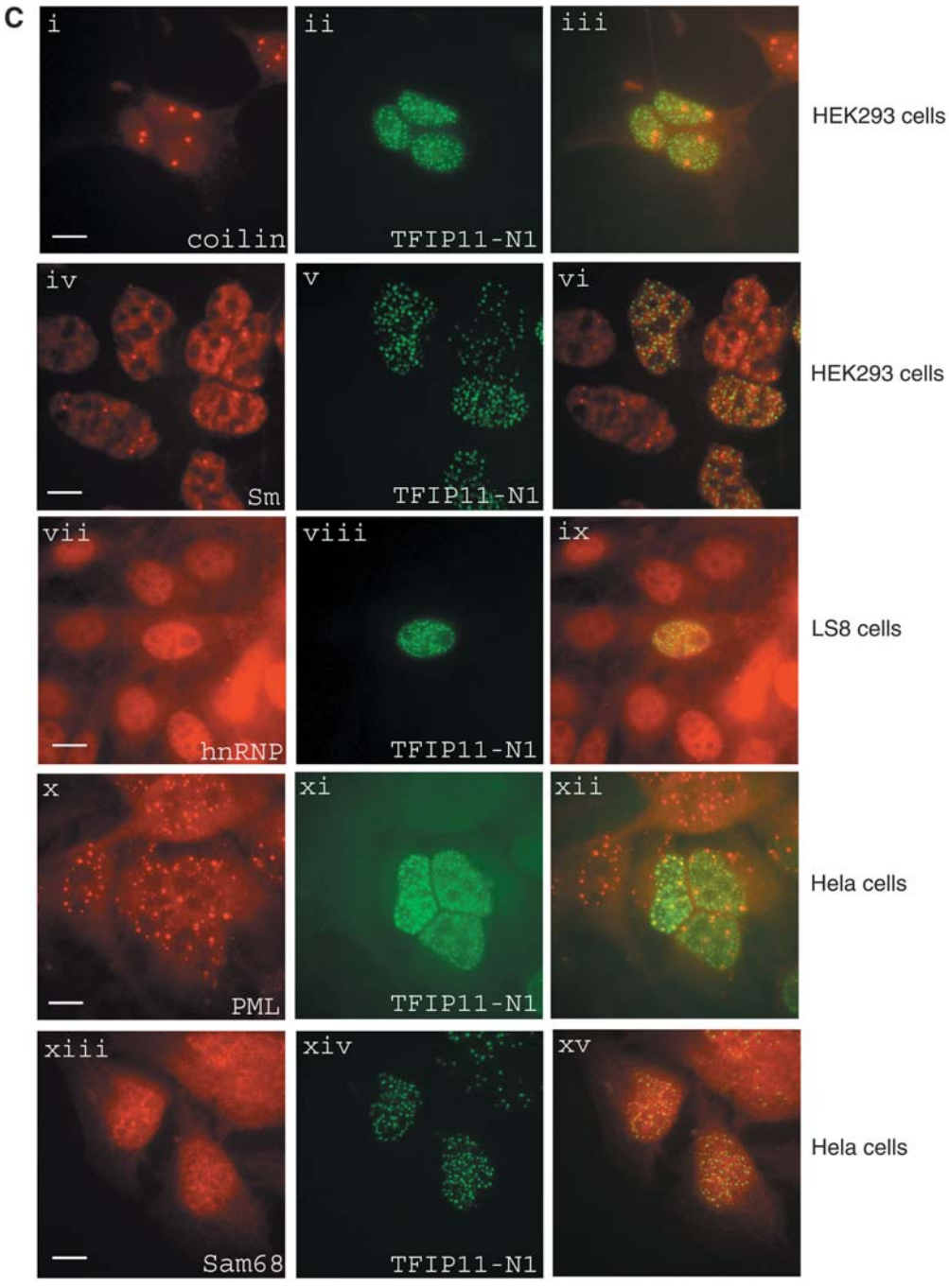

Figure 2 (continued)

olar compartment, the localization of their corresponding marker proteins (coilin, Sm antigen, RNP M3/M4, PML, or Sam68) were compared with that of transiently transfected TFIP11-N1 (fig. 2C). No colocalization was detected in any of those structures. These data suggested that the TFIP body represented a novel subnuclear structure.

The nuclear distribution of TFIP11 was sensitive to RNA polymerase II transcription

To examine whether the localization of the TFIP body was affected by ongoing gene expression that is known to alter other subnuclear structures, the subcellular localization of TFIP11 was studied in the presence of known transcriptional or translational inhibitors. Inhibition of RNA polymerase (pol) II transcription has been shown to cause the rounding up of splicing factor speckles [19]. To determine whether the nuclear localization of TFIP11 was

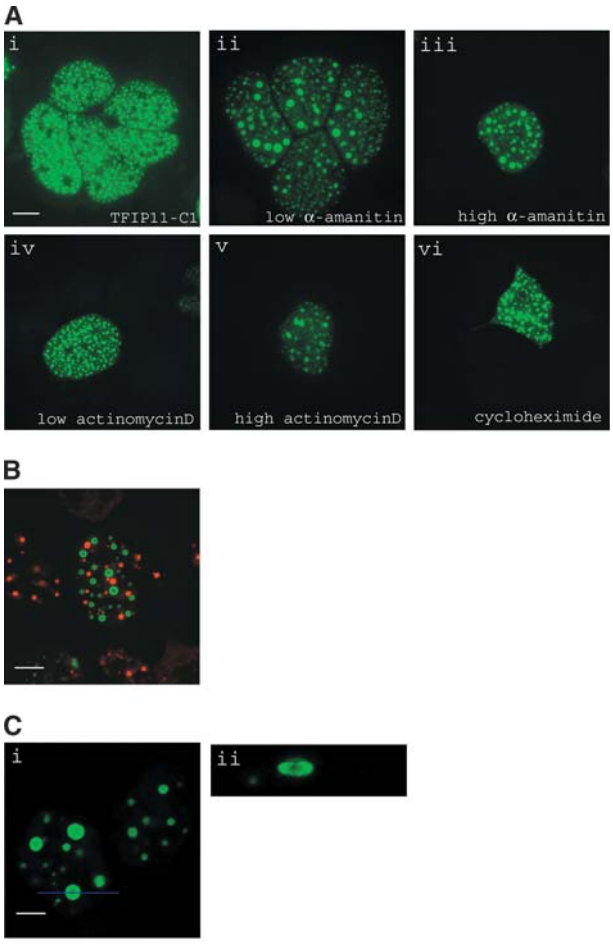

Figure 3. Effect of transcription and translation inhibition on the localization of TFIP11. Scale bar, 10 μm. (*A*) HEK293 cells were transiently transfected with TFIP11-C1 (i) and treated with 50 μg/ml α-amanitin for 5 h (ii), 300 μg/ml α-amanitin for 5 h (iii), 0.04 μg/ml actinomycin D for 3 h (iv), 50 μg/ml actinomycin D for 3 h (v) or 100 μg/ml cycloheximide for 5 h (vi). The images were taken from a fluorescent microscope. (*B*) After transient transfection with TFIP11-C1 and treatment with 50 μg/ml α-amanitin for 5 h, HEK293 cells were immunostained with antibody against SC35 and observed under a confocal microscope. (*C*) Confocal images of cells treated with 50 μg/ml α-amanitin for 5 h. The image in ii was taken from a cross section shown as a line in i and magnified twofold. All scale bars shown are 10 μm.

also sensitive to RNA pol II transcription inhibition, HEK293 cells were transiently transfected with TFIP11-C1 (fig. 3A) and subsequently treated with α-amanitin and actinomycin D. Treatment with α-amanitin at 50 μg/ml to inhibit RNA poly II transcription resulted in the rounding up of the TFIP body with increased size and reduced number (fig. 3A). Higher α-amanitin (300 μg/ml), which inhibits both pol II and pol III, showed no further effect (fig. 3A). Treatment with actinomycin D at 50 μg/ml, which inhibits all three RNA polymerases, gave rise to similar results as treatment with α-amanitin (fig. 3A). When a lower concentration of actinomycin D (0.04 μg/ ml) was used, in which only RNA poly I was expected to be blocked, no changes in the TFIP body were observed (fig. 3A). Incubation with cycloheximide had no effect (fig. 3A). These results indicated that, similar to splicing components such as SC35, the nuclear distribution of TFIP11 was sensitive to RNA pol II-mediated transcription and was independent of translation. The observation that upon transcription inhibition, the TFIP body became aggregated (bigger and fewer) suggested that it might be a storage/assembly/modification site, rather than the active site, of pre-messenger mRNA processing.

To determine whether TFIP bodies merge with nuclear speckles after inhibition of RNA poly II-mediated transcription, HEK293 cells were transiently transfected with TFIP11-C1, treated with α-amanitin (50 μg/ml), and immunostained with antibody against SC35. As shown in figure 3B, although both TFIP bodies and SC35 nuclear speckles rounded up, they were present in distinctive structures.

When cells treated with α-amanitin (50 μg/ml) were examined under confocal microscopy, TFIP11 was found to localize at the surface of a sphere (fig. 3C). This was further examined by observing the same sphere from a cross-section shown as a line in figure 3C. The image observed from the cross section showed an oblate spheroid with a hollow center (fig. 3C). Taken together, TFIP11 appeared to reside at the surface of the sphere-like structure of the TFIP body.

TFIP bodies were sensitive to RNase A treatment

Many nuclear substructures are involved in RNA processing. To determine whether TFIP11 was retained in the distinctive bodies in an RNA-dependent manner, HEK293 cells were transfected with TFIP11-C1 and treated with RNase A, and protein localization was examined by fluorescence microscopy. The distribution was dramatically changed after RNase A treatment: the typical TFIP body (fig. 4) became diffuse in the nucleoplasm with an increased number and reduced size of dots. This result suggested that the localization of TFIP11 in the TFIP body might be mediated by its association with RNA.

A role for TFIP11 in alternative splicing

When alternative splicing exists, the choice between the alternative sites depends on the relative quality of the constitutive signals, and regulatory proteins can shift this balance and favor the usage of one site. To investigate the potential role of TFIP11 in regulating pre-mRNA splicing, an in vivo splicing assay was performed. This assay is based on the notion that splice factors function in a dose-dependent manner influencing splice patterns of alternatively spliced genes [13, 20]. An adenovirus E1A minigene, capable of producing multiple mRNAs, was cotransfected into cells along with the TFIP11-EGFP fusion construct. The five major E1A mRNA isoforms

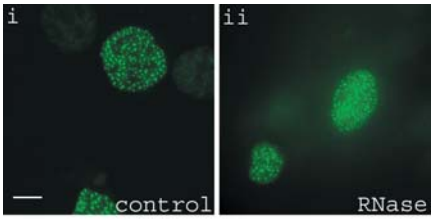

Figure 4. Effect of RNase A treatment on the localization TFIP11. HEK293 cells were transfected with TFIP11-C1, fixed with methanol and incubated with either PBS (i) or 100 μg/ml RNase A for 2 h (ii), followed by standard fluorescence microscopy. Scale bar, 10 μm, for both images.

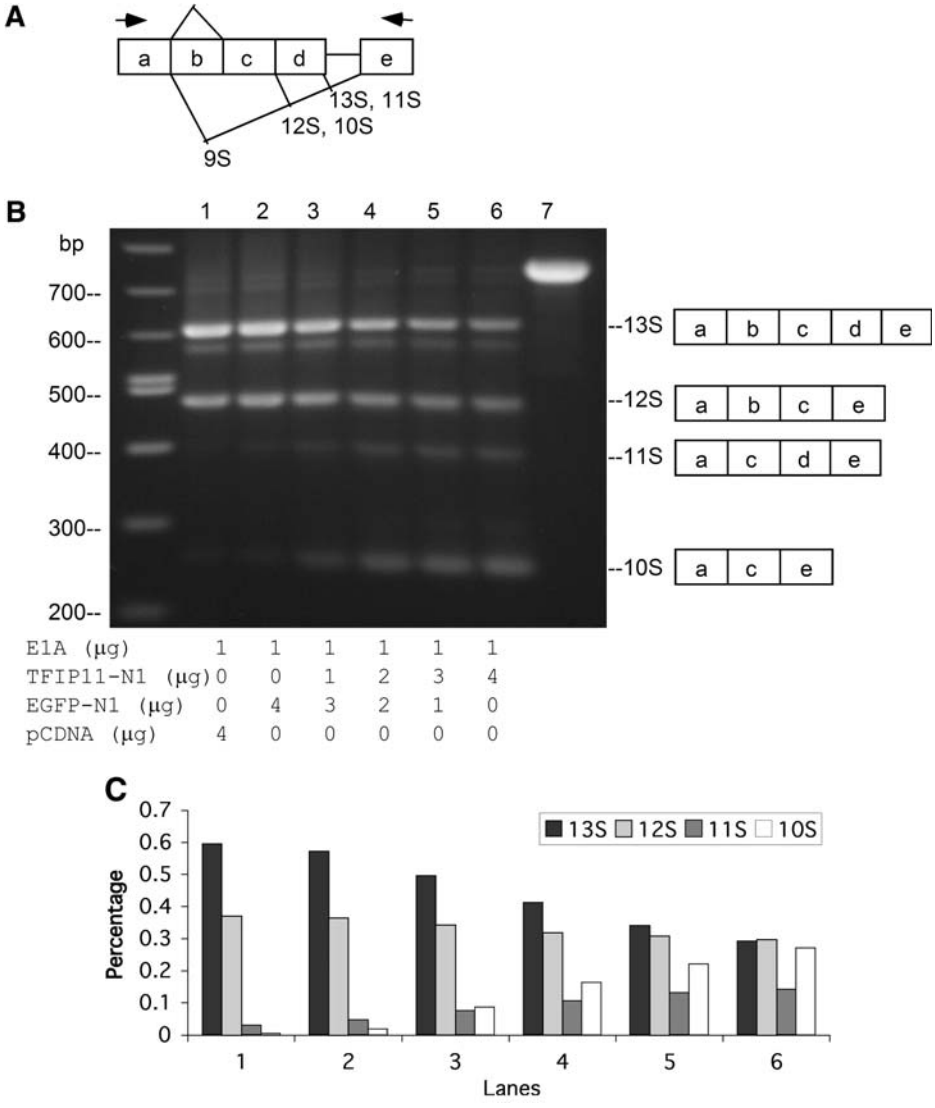

Figure 5. TFIP11 affected splicing of the adenovirus E1A minigene in LS8 cells. (*A*) Schematic representation of the E1A minigene structure and primers used for PCR. (*B*) Pattern of E1A alternative splicing in LS8 cells upon transfection of the minigene and cotransfection of TFIP11-EGFP expression vector. Left panel shows PCR products separated on an agarose gel. A total of 1 μg of the minigene E1A was added in each reaction. The concentration of TFIP11 protein was increased by adding 0, 1, 2, 3, 4 μg of its expression plasmid TFIP11-N1. The total amount of transfected DNA was kept constant by the addition of parental vector pEGFP-N1. A control with 1 μg of E1A and 4 μg of the empty pcDNA3 vector was also included in lane 1. The PCR control using plasmid E1A as template is shown in lane 7. Right panel shows the structure of the reaction products. (*C*) The 13S, 12S, 11S, and 10S mRNA isoforms were quantitated and the percentage of each isoform is shown.

(fig. 5A) are 13S, 12S, 11S, 10S, and 9S. The 13S, 12S, and 9S mRNA isoforms are generated by alternative 5′ splice site selection, while the 11S and 10S mRNAs are identical to the 13S and 12S mRNAs, except for an internal stretch (region b as shown in fig. 5A), which is removed by splicing as well [21]. In our case, transfection of the E1A minigene alone into LS8 cells generated four species of mRNA (13S, 12S, 11S, and 10S). Cotransfection of TFIP11-N1 resulted in an increase in the amount of 11S (5–14%) and 10S (2–29%) and a decrease in the 13S (57–29%) and 12S (36–30%) in a dose-dependent manner (fig. 5B, C). The expression of TFIP11 caused a shift toward use of the double splicing events, which is characteristic of the adenovirus late stage of infection [21]. These results also demonstrate a clear relationship between TFIP11 expression levels and splicing.

Discussion

In this study we show that TFIP11 is a likely RNA splicing factor that forms distinctive dot-like structures in the nucleus. We refer to each of these structures as the TFIP body. The TFIP bodies lie close to, but do not overlap with SC35 nuclear speckles. An in vivo splicing assay demonstrated that TFIP11 is involved in splicing. Careful examination of other distinct structures within the nucleus, such as Cajal bodies, PML, and Sm, suggests that the TFIP body may be a novel subnuclear structure. No colocalization of TFIP11 and paraspeckles was observed, which likely reflects the distinct and unrelated expression profiles observed previously for paraspeckles and SC35 [16]. Although the existence of distinct nuclear compartments is now well established, the function of most of them is far from clear. The finding that a splicing factor forms a novel subnuclear structure reveals a new level of structural and functional complexity in the nucleus.

Like the SC35 speckles, TFIP bodies tend to enlarge and round up in response to inhibitors of RNA poly II including α-amanitin and actinomycin D [19]. For unknown reasons, another pol II inhibitor DRB had no effect (unpublished data). This sensitivity to RNA poly II-mediated transcription is consistent with the nuclear localization pattern for many proteins, and this pattern has been shown to change during the cell cycle and in response to changes in cellular metabolic activity [17, 22]. Clustering of splicing factors has been suggested to result from the accumulation of splicing components at storage sites in response to a reduction in pre-mRNA levels [11]. This points to the idea that instead of being the active splicing sites, TFIP bodies function as storage and/or assembly compartments that can supply TFIP11 to active transcription/splicing sites. One emerging model from this study is that splicing components may be stored at different subnuclear structures other than the SC35 splicing speckles, and both storage structures are in close proximity to the active transcription sites so that the components can be quickly recruited to the active sites upon sensing signals. When there is no active transcription, these structures tend to cluster. TFIP11 is highly phosphorylated (unpublished data), and the phosphorylation and dephosphorylation may represent an underlying mechanism that drives the movement of TFIP11 between the active splicing sites and the storage sites.

Although nuclear localization signals for nuclear uptake of proteins are well characterized [23], signals for specific subnuclear distribution are still largely unknown. The RS domain of SR proteins and TP domain of spliceosomal protein SF3b155 are believed to direct the specific SC35 speckle localization [24, 25]. On the other hand, several studies have suggested that targeting a protein to a specific subnuclear structure results from protein-protein interactions with other components within the structure. A single localization signal does not exist for subnuclear compartments such as Cajal bodies and nucleoli [26, 27]. The most striking feature of the observed TFIP bodies is the accumulation of the protein in round nuclear dots that number between 20 and 150, and these are excluded from nucleoli. The number and size of of TFIP body are independent of the intracellular concentration of TFIP11 (unpublished data). Deletion and mutation analyses will further help to understand the mechanism of the unique localization TFIP bodies, either due to simple sequence motif-mediated events or protein-protein interaction.

The implication of TFIP11 in splicing helps to decipher the spliceosome, which is to date the most complex functional machinery characterized in cells [4]. The human genome project reveals that there are far fewer genes in the genome than expected. However, the majority of premessengers are alternatively spliced, possibly to generate functional diversity. Splicing represents a key step in the control of protein function in a large variety of biological systems. Our finding of TFIP11 as a component of the spliceosome is important for an eventual understanding of how splicing factors and small nuclear RNAs are stored and assembled into a spliceosome, and ultimately how splicing events are regulated.

Acknowledgements. We are grateful to Dr. S. Stamm for generously providing us with minigene constructs, and Drs. A. Lamond and A. Fox for generously providing a polyclonal antibody to paraspeckle protein 1 (PSP1). The authors would like to thank P. Bringas Jr., M. MacVeigh, and Dr. W. Luo for helping with the fluorescence and confocal microscopy, H. J. Wang, C. Martin, Dr. D. Zhu, and Y. Xu for their expert technical assistance throughout this study, and B. Yoshida and Dr. C. Paine for help editing the manuscript. The confocal microscope used for this study was provided by the Microscopy Sub Core at the USC Center for Liver Disease (NIH 1 P30 DK48522). This work was supported by grants DE13404 and DE14867 from the National Institute of Dental and Craniofacial Research.

1 Paine C. T., Paine M. L., Luo W., Okamoto C. T., Lyngstadaas S. P. and Snead M. L. (2000) A tuftelin-interacting protein (TIP39) localizes to the apical secretory pole of mouse ameloblasts. J. Biol. Chem. **275:** 22284–22292
2 Deutsch D., Palmon A., Catalano-Sherman J. and Laskov R. (1987) Production of monoclonal antibodies against enamelin and against amelogenin proteins of developing enamel matrix. Adv. Dent. Res. **1:** 282–288
3 Mao Z., Shay B., Hekmati M., Fermon E., Taylor A., Dafni L., et al. (2001) The human tuftelin gene: cloning and characterization. Gene. **279:** 181–196
4 Zhou Z., Licklider L. J., Gygi S. P. and Reed R. (2002) Comprehensive proteomic analysis of the human spliceosome. Nature **419:** 182–185
5 Jurica M. S. and Moore M. J. (2003) Pre-mRNA splicing: awash in a sea of proteins. Mol. Cell **12:** 5–14
6 Clayton R. A., White O., Ketchum K. A. and Venter J. C. (1997) The first genome from the third domain of life. Nature **387:** 459–462
7 Matera A. G. (1999) Nuclear bodies: multifaceted subdomains of the interchromatin space. Trends Cell Biol. **9:** 302–309
8 Lamond A. I. and Earnshaw W. C. (1998) Structure and function in the nucleus. Science **280:** 547–553
9 Sleeman J. E. and Lamond A. I. (1999) Nuclear organization of pre-mRNA splicing factors. Curr. Opin. Cell Biol. **11:** 372–377
10 Hastings M. L. and Krainer A. R. (2001) Pre-mRNA splicing in the new millennium. Curr. Opin. Cell Biol. **13:** 302–309
11 Lamond A. I. and Spector D. L. (2003) Nuclear speckles: a model for nuclear organelles. Nat. Rev. Mol. Cell Biol. **4:** 605–612
12 Kambach C., Walke S. and Nagai K. (1999) Structure and assembly of the spliceosomal small nuclear ribonucleoprotein particles. Curr. Opin. Struct. Biol. **9:** 222–230
13 Stoss O., Stoilov P., Hartmann A. M., Nayler O. and Stamm S. (1999) The in vivo minigene approach to analyze tissue-specific splicing. Brain Res. Brain Res. Protoc. **4:** 383–394
14 Paine C. T., Paine M. L. and Snead M. L. (1998) Identification of tuftelin- and amelogenin-interacting proteins using the yeast two-hybrid system. Connect. Tissue Res. 38: 257–267
15 Zhou Y. L. and Snead M. L. (2000) Identification of CCAAT/enhancer-binding protein alpha as a transactivator of the mouse amelogenin gene. J. Biol. Chem. **275:** 12273–12280
16 Fox A. H., Lam Y. W., Leung A. K. L., Lyon C. E., Andersen J., Mann M. et al. (2002) Paraspeckles: a novel nuclear domain. Curr. Biol. **12:** 13–25
17 Nayler O., Hartmann A. M. and Stamm S. (2000) The ER repeat protein YT521-B localizes to a novel subnuclear compartment. J. Cell Biol. **150:** 949–962
18 Fu X. D. and Maniatis T. (1992) The 35-kDa mammalian splicing factor SC35 mediates specific interactions between U1 and U2 small nuclear ribonucleoprotein particles at the 3′ splice site. Proc. Natl. Acad. Sci. USA **89:** 1725–1729
19 Spector D. L., Landon S. and O'Keefe R. T. (1993) Organization of RNA polymerase II transcription and pre-mRNA splicing within the mammalian cell nucleus. Biochem. Soc. Trans. **21:** 918–920
20 Caceres J. F., Stamm S., Helfman D. M. and Krainer A. R. (1994) Regulation of alternative splicing in vivo by overexpression of antagonistic splicing factors. Science **265:** 1706–1709
21 Stephens C. and Harlow E. (1987) Differential splicing yields novel adenovirus 5 E1A mRNAs that encode 30 kd and 35 kd proteins. EMBO J. **6:** 2027–2035
22 Dostie J., Lejbkowicz F. and Sonenberg N. (2000) Nuclear eukaryotic initiation factor 4E (eIF4E) colocalizes with splicing factors in speckles. J. Cell Biol. **148:** 239–247
23 Moroianu J. (1999) Nuclear import and export pathways. J. Cell Biochem. **Suppl 32–33:** 76–83
24 Fu X. D. (1995) The superfamily of arginine/serine-rich splicing factors. RNA. **1:** 663–680
25 Eilbracht J. and Schmidt-Zachmann M. S. (2001) Identification of a sequence element directing a protein to nuclear speckles. Proc. Natl. Acad. Sci. USA **98:** 3849–3854
26 Zirwes R. F., Kouzmenko A. P., Peters J. M., Franke W. W. and Schmidt-Zachmann M. S. (1997) Topogenesis of a nucleolar protein: determination of molecular segments directing nucleolar association. Mol. Biol. Cell **8:** 231–248
27 Bohmann K., Ferreira J. A. and Lamond A. I. (1995) Mutational analysis of p80 coilin indicates a functional interaction between coiled bodies and the nucleolus. J. Cell Biol. **131:** 817–831